Silicon (2019) 11:1313–1326
https://doi.org/10.1007/s12633-018-9924-y

ORIGINAL PAPER

# Statistical Analysis and Optimization of Process Parameters in Wire Cut Machining of Welded Nanostructured Hardfacing Material

Abhijit Saha[1] · Subhas Chandra Mondal[2]

Received: 19 May 2017 / Accepted: 1 June 2018 / Published online: 5 July 2018



## Abstract

Wire electric discharge machining (WEDM) is a nontraditional machining technique to cut hard and conductive material with the assistance of a moving electrode. Nanostructured hardfacing material is a hard alloy with high hardness and wear resisting property. The motivation behind this research is to explore the impact of parameters on material removal rate, surface roughness and machining time for WEDM using welded nanostructured hardfacing material as work piece. The hardfacing layer was prepared by manual metal arc welding (MMAW). Taguchi's L25 orthogonal array was utilized to design the investigational runs. Different hardfaced layer thicknesses were examined to bring out the influence of hardfacing on WEDM performances. Moreover, Multi-objective optimization was carried out using TOPSIS and PCA to recognize optimal process parameters. Optimum combination of input process parameters for the multiple performance characteristics should be preferred as $A_1B_5C_5D_5E_5$ (brass wire) and $A_2B_3C_4D_5E_1$ (Zinc coated brass wire).


**Keywords** WEDM · Hardfacing · MMAW · TOPSIS · PCA

## 1 Introduction

A huge segment of the designing applications require excellent dimensional accuracy, wear and corrosion free materials for their extended trustworthiness. Numerous enterprizes confront the issues from wearing out components which were being used even under proper service conditions. Because of continuous and gradual wear, the components become useless and need frequent replacement which results in increment of product cost. To conquer these troubles, the exploration for the advancement on the execution of the hardfacing materials has been altogether enhanced in the most recent couple of decades [1, 2]. Hardfacing is prominent amid the various strategies to reduce the costs on the upkeep front and also to improve unwavering quality of the equipment. The productivity of the hardfacing procedure relies on the preference of the materials and its element proportion for distinct designing applications.

Nowadays, nano-composite hardfacing material has pick up extending thought for its significant assurance contrary to thermal impact, abrasion and corrosion. Nano-particle coating is able to improve the mechanical properties of the matrix by more sufficiently propelling the molecule solidifying mechanisms than micron estimate particles [3]. The quality of the material in the nanostructured state is a few times higher in correlation with the traditional coarse-crystalline material [4]. Machining of these alloys are very difficult through conventional machining because conventional machining may affect their internal properties, therefore non-traditional machining methods are more suitable for machining of such kind of materials [5, 6]. WEDM process is thought to be the best option strategy for machining hardfacing materials. In wire EDM, the spark jumps from the wire electrode to the workpiece and erodes metal both from the workpiece and wire electrode and the flowing dielectric flushes away the debris. Electric discharge causes the melting and vaporization of materials by pulsed direct current between the wire electrode and

✉ Abhijit Saha
alfa.nita2010@gmail.com

1 Production Engineering Department, Haldia Institute of Technology, Haldia 721657, India

2 Mechanical Engineering Department, Indian Institute of Engineering Science and Technology, Shibpur 711103, India

the workpiece [7–9]. In literature, WEDM is generally relevant for machining extensive ranges of materials under various machining conditions [10–21]. However, limited or no research has been reported on nano-structured hardfacing material. The material is suitable on WEDM as it is conductive and hard. In view of these attributes, it has numerous applications in aviation and mining businesses.

Several researchers and practioners applied Taguchi's experimental design and ANOVA techniques as an efficient tool for interpreting the effect of input process criterion on responses in manufacturing processes [22–24]. Bhangoria et al. [22] used the statistical and regression analysis of kerf width using Taguchi's L32 orthogonal array method. ANOVA technique was used to get the process parameters affecting the kerf width. Tosun [23] used regression analysis to scrutinize the impact of cutting parameters on wire crater. In another review, Tosun et al. [24] advanced the machining exhibitions of kerf and MRR using S/N ratio. The mathematical models utilized for improvements were produced by regression analysis. Ahmed and Kumar [25] used TOPSIS method to obtain best optimal combinations in cryogenic drilling on Ti-6Al-4V alloy. Kalayarasan and Murali [26] applied Taguchi GRA and TOPSIS used to optimize the process parameter in EDM of ceramic composites. Şimşek et al. [27] proposed a TOPSIS-based Taguchi optimization to determine optimal mixture proportions of the high strength self-compacting concrete.

Effective usage of WEDM is fundamental to choose most appropriate machining conditions for to value cutting proficiency and grow top notch machined parts at least preparing cost. The systems utilized for optimizing process parameters by methods for test techniques and numerical models have expanded significantly with time to finish a general goal of improving profitability and propelling cutting procedure productivity. It is found though, from the machining literature that a very few authors [28, 29], examined the effects of various input process parameters on performance characteristics in WEDM for machining nanostructured hardfacing material. No study has been available on statistical analysis of quality characteristics and effect of hardfaced layer thickness on WEDM performance.

According to the surveyed literature, advantages and disadvantages of the above works were clarified; thus, in the present study, main objective is to statistically analyze the experimental results through Taguchi and ANOVA technique. Furthermore, influence of different hardfaced layer thickness was also investigated on WEDM performance characteristics. This involvement is applicable for both manufacturing and educational benefit. Finally, a hybrid approach i.e. TOPSIS methods in combination with PCA have been used to recognize optimum parametric combinations.

## 2 Experimental Procedure

### 2.1 Work Material

There is a rising demand for high hardness and high abrasive wear resistance materials which give superior performance under severe conditions. Tubular coated nano-technology based electrode was used for the hardfacing purpose [28]. The manual metal arc welding assisted hardfacing was done on the substrate material. Figure 1 shows the present work sample.

### 2.2 Equipment and Specimens

A no. of experiments has been undergone on 5-axis WT 355 CNC WEDM machine. A 0.25 mm diameter of Brass wire [60–63% Cu and balance Zn] and zinc-coated brass wire electrode [consists of 5 $\mu$m zinc coating over a standard brass wire] have been chosen. The size of the work piece considered for experimentation is 90 mm width, 65 mm length and 13 mm depth of cut. Furthermore, for each set of cutting parameters, the work piece was cut with a length of 12.7 mm (Fig. 2).

### 2.3 Experimental Parameters and Design

As it is known, the WEDM process is an unconventional machining process in which many factors affect on its performance. The most prominent parameters in WEDM process include discharge stop time (factor A), discharge pulse time (factor B), wire tension (factor C), servo voltage (factor D) and the wire feed rate (factor E). Likewise, process quality measure includes MRR, surface roughness and machining time. In this work five input process parameters have been selected at five levels and shown in Table 1. The experiments were conducted with fixed values of arc on time ($A_{on} = 8$ unit), arc off time ($A_{off} = 10$ unit),

**Fig. 1** Hardfacing coating after welding

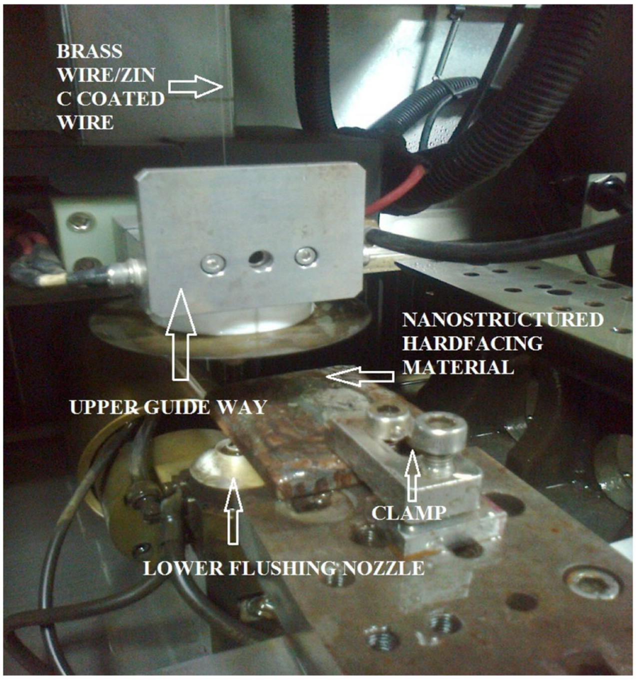


**Fig. 2** Photograph of machining operation [29]

open voltage (OV = 8 unit) and water flow rate (WA = 7unit). L25 Taguchi's orthogonal array is employed for the experimentation [29].

## 2.4 Performance Evaluation

In the present work the cutting performance of WEDM is measured by using three important responses i.e. MRR, machining time and surface roughness ($R_a$). A total of 25 (fractional factorial of level$^{5-3}$) experiments were planned and performed according to the experimental layout. MRR for WEDM operation was calculated using Eq. 7:

$$\text{MRR} = \text{CsL} \tag{1}$$

where Cs and L are the cutting speed and thickness of the material.

To determine surface roughness of WEDMed specimens Mitutoyo Surftest SJ-301 surface profile meter was used. For 3 mm hardfaced layer thickness, experimental outcome are given in Table 2.

# 3 TOPSIS Method

In this research work, a MCDM model [30] specifically TOPSIS [25–27] has been exploited for the optimization of several responses. The course of action is given below:

**Step 1:** Formation of decision matrix

$$D \begin{bmatrix} \eta_{11} & \eta_{12} & \cdots\cdots & \eta_{1n} \\ \eta_{21} & \eta_{22} & \cdots\cdots & \eta_{2n} \\ \cdots\cdots & \cdots\cdots & \cdots\cdots & \cdots\cdots \\ \eta_{m1} & \eta_{m2} & \cdots\cdots & \eta_{mn} \end{bmatrix} \tag{2}$$

**Step 2:** Computation of normalized ratings by the vector normalization:

$$r_{ij} = \frac{\eta_{ij}}{\sqrt{\sum_{i=1}^{m} \eta_{ij}^2}} \tag{3}$$

Where, $r_{ij}$ denotes the normalized value i-th alternative on j-th criterion.

**Step 3:** Appraisal of weight using PCA

Computation of correlation coefficient derived from Eq. 6:

$$R_{jl} = \left( \frac{\text{cov}(x_i(j), x_i(l))}{\sigma x_i(j) * \sigma x_i(l)} \right) \tag{4}$$

$$(R - \lambda_x I_m)\, V_{ik} = 0 \tag{5}$$

Where $\lambda_x$ eigenvalues, and $V_{ik}$ is the Eigen vectors

Thus, the principal components are:

$$Y_{mk} = \sum_{i=1}^{n} x_m(i) V_{ik} \tag{6}$$

Where $Y_{mk}$ is known as principal components

**Table 1** Machining parameter with their levels [29]

| Machining parameter | Factor | Unit | Level 1 | Level 2 | Level 3 | Level 4 | Level 5 |
|---|---|---|---|---|---|---|---|
| Discharge pulse time ($T_{on}$) | A | $\mu$s | 0.3 | 0.35 | 0.4 | 0.45 | 0.5 |
| Discharge stop time ($T_{off}$) | B | $\mu$s | 8 | 9 | 10 | 11 | 12 |
| Servo voltage ($SV$) | C | V | 35 | 38 | 41 | 44 | 47 |
| Wire tension ($WT$) | D | g | 500 | 600 | 700 | 800 | 900 |
| Wire feed rate ($WF$) | E | m/min | 5 | 6 | 7 | 8 | 9 |

**Table 2** L25 orthogonal array depicting the parameter levels and responses [29]

| Expt No. | Parameter levels | | | | | Responses | | | | | |
|---|---|---|---|---|---|---|---|---|---|---|---|
| | | | | | | Brass wire | | | Zinc coated brass wire | | |
| | A | B | C | D | E | MRR | Machining time | $R_a$ | MRR | Machining time | $R_a$ |
| 1 | 1 | 1 | 1 | 1 | 1 | 39.434 | 2.56 | 3.06 | 39.321 | 2.57 | 2.83 |
| 2 | 1 | 2 | 2 | 2 | 2 | 31.628 | 3.53 | 3.20 | 36.322 | 3.15 | 2.74 |
| 3 | 1 | 3 | 3 | 3 | 3 | 30.407 | 4.00 | 2.69 | 36.635 | 3.35 | 3.00 |
| 4 | 1 | 4 | 4 | 4 | 4 | 27.008 | 4.50 | 2.21 | 33.204 | 3.56 | 2.61 |
| 5 | 1 | 5 | 5 | 5 | 5 | 24.174 | 5.18 | 2.59 | 27.683 | 4.30 | 2.70 |
| 6 | 2 | 1 | 2 | 3 | 4 | 32.911 | 3.34 | 2.70 | 36.549 | 3.10 | 3.17 |
| 7 | 2 | 2 | 3 | 4 | 5 | 35.724 | 3.28 | 2.65 | 42.238 | 2.42 | 3.49 |
| 8 | 2 | 3 | 4 | 5 | 1 | 30.808 | 4.20 | 2.19 | 35.541 | 4.05 | 2.73 |
| 9 | 2 | 4 | 5 | 1 | 2 | 28.241 | 4.31 | 2.39 | 37.908 | 3.50 | 2.45 |
| 10 | 2 | 5 | 1 | 2 | 3 | 29.933 | 3.51 | 2.62 | 33.075 | 3.20 | 2.68 |
| 11 | 3 | 1 | 3 | 5 | 2 | 41.943 | 3.01 | 2.79 | 45.044 | 3.00 | 2.59 |
| 12 | 3 | 2 | 4 | 1 | 3 | 39.045 | 3.07 | 2.09 | 41.118 | 2.40 | 2.73 |
| 13 | 3 | 3 | 5 | 2 | 4 | 35.708 | 4.57 | 2.67 | 41.533 | 2.20 | 2.60 |
| 14 | 3 | 4 | 1 | 3 | 5 | 36.217 | 3.45 | 2.72 | 36.016 | 3.12 | 2.55 |
| 15 | 3 | 5 | 2 | 4 | 1 | 37.821 | 3.2 | 2.80 | 36.352 | 3.10 | 2.90 |
| 16 | 4 | 1 | 4 | 2 | 5 | 32.676 | 3.37 | 2.47 | 42.803 | 2.49 | 3.34 |
| 17 | 4 | 2 | 5 | 3 | 1 | 41.171 | 3.00 | 2.93 | 46.563 | 3.34 | 3.10 |
| 18 | 4 | 3 | 1 | 4 | 2 | 48.768 | 2.29 | 2.78 | 52.125 | 3.00 | 3.25 |
| 19 | 4 | 4 | 2 | 5 | 3 | 43.911 | 2.44 | 2.80 | 50.970 | 2.05 | 2.73 |
| 20 | 4 | 5 | 3 | 1 | 4 | 36.239 | 3.36 | 2.88 | 43.862 | 2.35 | 2.86 |
| 21 | 5 | 1 | 5 | 4 | 3 | 50.388 | 2.28 | 2.80 | 52.360 | 2.01 | 2.86 |
| 22 | 5 | 2 | 1 | 5 | 4 | 47.162 | 2.50 | 3.18 | 43.237 | 2.44 | 2.58 |
| 23 | 5 | 3 | 2 | 1 | 5 | 39.999 | 3.08 | 2.68 | 61.055 | 1.45 | 2.87 |
| 24 | 5 | 4 | 3 | 2 | 1 | 48.536 | 2.38 | 3.57 | 52.469 | 1.51 | 2.47 |
| 25 | 5 | 5 | 4 | 3 | 2 | 45.841 | 2.27 | 6.45 | 49.369 | 2.15 | 2.74 |

**Step 4:** Compute the weighted normalized decision matrix.

$$\mathbf{v}_{ij} = \mathbf{r}_{ij} \times \mathbf{w}_j \tag{7}$$

where $w_j$ is the weightage

**Step 5:** Establish the ideal ($A^*$) and negative ideal ($A^-$) solutions.

$$A^* = \left\{ \left( \max_i v_{ij} | j \in C_b \right), \left( \min_i v_{ij} | j \in C_c \right) \right\} = \{ v_{ij}^* | j = 1, 2, ..., m \} \tag{8}$$

$$\bar{A} = \left\{ \left( \min_i v_{ij} | j \in C_b \right), \left( \max_i v_{ij} | j \in C_c \right) \right\} = \{ v_j^- | j = 1, 2, ..., m \} \tag{9}$$

**Step 6:** Evaluate the separation measures using the m-dimensional Euclidean distance.

$$S_i^* = \sqrt{\sum_{j=1}^{m} (v_{ij} - v_j^*)^*} \tag{10}$$

$$S_i^- = \sqrt{\sum_{j=1}^{m} (v_{ij} - v_j^-)^2} \tag{11}$$

Where $j = 1, 2, ..., m$

**Step 7:** Calculate the relative closeness to the ideal solution.

$$RC_i^* = \frac{S_i^-}{S_i^* + S_i^-} \quad i = 1, 2, ..., m \tag{12}$$

**Step 8:** Rank the preference order

### 3.1 Optimization Results: TOPSIS – PCA Hybrid Approach

Individual weightage of each quality characteristics were evaluated using PCA according to Eq. 5. The contributions are 0.392, 0.399, and 0.209 (for brass wire), for zinc coated brass wire, 0.496, 0.480 and 0.025, respectively. Weighted normalized values are determined using Eq. 7. Subsequently, positive ideal solution ($A^*$) and negative ideal solutions (A) were calculated using Eqs. 8 and 9. Finally, Eq. 12 is used to calculate the similarity of the ideal solutions in each scenario (Table 5). It was obtain that test no. 5 (for brass wire) and 8 (zinc coated wire) have the maximum $RC_i^*$ value. Thus optimum combination of process parameters should be chosen as $A_1B_5C_5D_5E_5$ (brass wire), namely discharge pulse time 0.3 $\mu$s (level 1), discharge stop time 12 $\mu$s (level 5), servo voltage 47 V (level 5), wire tension 900 g (level 5) and wire feed rate 9 m/min (level 5). Correspondingly, for zinc coated brass wire ($A_2B_3C_4D_5E_1$), the optimal settings are discharge pulse time 0.35 $\mu$s (level 2), discharge stop time 10 $\mu$s (level 3), servo voltage 44 V (level 4), wire tension 900 g (level 5) and wire feed rate 5 m/min (level 1). Same best possible amalgamation of process parameters has been found for 4 mm hardfacing layer thickness also (Table 3).

At optimized process parameters microstructure analysis has been carried out on machined surface. Micro holes, cracks, small debris and blow holes were noticed on the machined surface which is seen in Fig. 3. Only a few micro holes and melted debris were observed because of the low discharge energy which thus offers a smooth surface on the machined components.

## 4 Results and Discussions

### 4.1 Statistical Analysis

Each experiment was conducted by varying input process parameters and the investigational data was statistically evaluated by ANOVA in conjunction with MINITAB

**Table 3** Closeness coefficient values and ranking of alternatives

| Experiment No. | Brass wire | | | | Zinc coated brass wire | | | |
|---|---|---|---|---|---|---|---|---|
| | $S_i^*$ | $S_i^-$ | $RC_i^*$ | Rank | $S_i^*$ | $S_i^-$ | $RC_i^*$ | Rank |
| 1 | 0.056 | 0.020 | 0.265 | 22 | 0.049 | 0.222 | 0.818 | 14 |
| 2 | 0.039 | 0.035 | 0.468 | 7 | 0.032 | 0.179 | 0.848 | 8 |
| 3 | 0.040 | 0.040 | 0.495 | 5 | 0.027 | 0.164 | 0.859 | 6 |
| 4 | 0.046 | 0.046 | 0.501 | 3 | 0.024 | 0.155 | 0.866 | 4 |
| 5 | 0.040 | 0.056 | 0.585 | 1 | 0.021 | 0.145 | 0.873 | 2 |
| 6 | 0.046 | 0.029 | 0.381 | 12 | 0.033 | 0.183 | 0.845 | 10 |
| 7 | 0.047 | 0.028 | 0.369 | 14 | 0.055 | 0.234 | 0.811 | 17 |
| 8 | 0.046 | 0.042 | 0.472 | 6 | 0.015 | 0.124 | 0.889 | 1 |
| 9 | 0.043 | 0.043 | 0.501 | 4 | 0.023 | 0.152 | 0.868 | 3 |
| 10 | 0.046 | 0.031 | 0.403 | 11 | 0.032 | 0.179 | 0.848 | 7 |
| 11 | 0.049 | 0.025 | 0.337 | 18 | 0.035 | 0.186 | 0.843 | 13 |
| 12 | 0.057 | 0.023 | 0.285 | 21 | 0.055 | 0.235 | 0.809 | 18 |
| 13 | 0.037 | 0.049 | 0.569 | 2 | 0.063 | 0.252 | 0.799 | 20 |
| 14 | 0.044 | 0.031 | 0.413 | 9 | 0.033 | 0.182 | 0.846 | 9 |
| 15 | 0.047 | 0.028 | 0.371 | 13 | 0.034 | 0.183 | 0.845 | 11 |
| 16 | 0.049 | 0.028 | 0.365 | 15 | 0.052 | 0.228 | 0.814 | 15 |
| 17 | 0.048 | 0.026 | 0.347 | 16 | 0.025 | 0.157 | 0.864 | 5 |
| 18 | 0.064 | 0.019 | 0.229 | 25 | 0.034 | 0.184 | 0.845 | 12 |
| 19 | 0.060 | 0.018 | 0.230 | 24 | 0.069 | 0.263 | 0.792 | 22 |
| 20 | 0.044 | 0.030 | 0.410 | 10 | 0.057 | 0.239 | 0.807 | 19 |
| 21 | 0.064 | 0.020 | 0.235 | 23 | 0.071 | 0.267 | 0.789 | 23 |
| 22 | 0.056 | 0.023 | 0.290 | 20 | 0.054 | 0.232 | 0.812 | 16 |
| 23 | 0.050 | 0.025 | 0.337 | 17 | 0.101 | 0.319 | 0.758 | 25 |
| 24 | 0.057 | 0.026 | 0.315 | 19 | 0.098 | 0.313 | 0.762 | 24 |
| 25 | 0.055 | 0.047 | 0.459 | 8 | 0.065 | 0.255 | 0.797 | 21 |

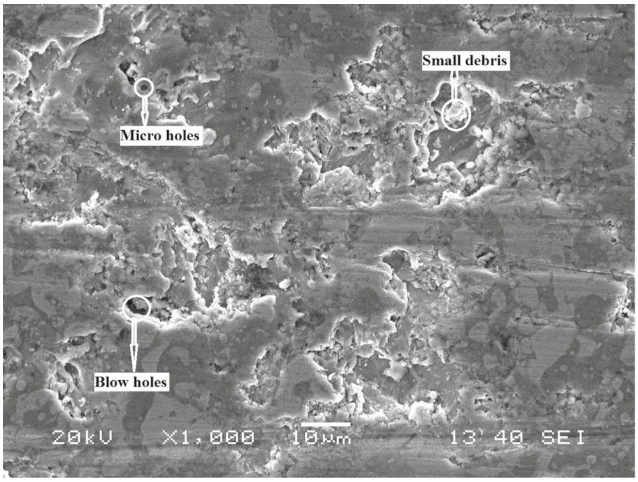


**Fig. 3** Microstructure analysis of machined surface

software. Precisely to survey the excellence attribute of the conduct test, the S/N ratios [$\eta$ (dB)] are considered.

$\eta$ (dB) value for HB performance (MRR):

$$\eta = -10\log_{10}\left[\frac{1}{n}\sum\nolimits_{i=1}^{n}\frac{1}{y_{i^2}}\right] \tag{13}$$

$\eta$ (dB) value for LB performance (machining time, $R_{a)}$:

$$\eta = -10\log_{10}\left[\frac{1}{n}\sum\nolimits_{i=1}^{n} y_i^2\right] \tag{14}$$

Where i = 1, 2 . . . .n,

It is perceived from Fig. 4a that optimal process parameters for the maximum MRR (brass wire) was A1B1C1D4E1 namely, discharge pulse time at 0.3 $\mu$s, discharge stop time at 8 $\mu$s, servo voltage at 35V, wire tension at 800 g and wire feed rate at 5 m/min. In the same way, for zinc coated brass wire, the consequent optimal settings are discharge pulse time of 0.3 $\mu$s (level 1), discharge stop time of 10 $\mu$s (level 3), servo voltage of 41 V (level 3), wire tension of 500 g (level 1) and wire feed rate of 6 m/min (level 2). Figure 4b and c represents the interactions between the process parameters which affect the material removal rate.

Figure 5a and b show Box–Cox plot for MRR which are used to determine the power transform for the performance characteristics. From Fig. 5a, it is practical that the estimated assessment of lambda is 0.10 and the rounded value (0.00), which is the value used in the transformation. It also includes the upper CL (2.24) and lower CL (−1.56), which are marked on the graph by vertical lines. In this graph (Fig. 5a) corresponds to an interval of −1.56 to 2.24. Similarly, Fig. 5b shows Box–Cox plot for MRR in case of zinc coated brass wire. Same statistical analysis can be done for other performance characteristics viz. machining time and surface roughness.

From ANOVA results (Table 4), it is pragmatic that discharge pulse time is the major influencing parameter for both the wires. Similar ANOVA analysis may be done for machining time and surface roughness, respectively.

Regression coefficients of the second-order equation are obtained by via trial data. The regression equations for performance characteristics are as follows:

$$\begin{aligned} MRR_{Brass\ wire} = {} & 173 - 230\,A + 13.7\,B - 5.59\,C - 0.1021\,D \\ & - 3.9\,E + 85\,A*A - 0.944\,B*B \\ & + 0.0155\,C*C + 0.000061\,D*D - 0.074\,E \\ & *E + 8.20\,A*B + 5.83\,A*C + 0.100\,A \\ & *D - 20.02\,A*E - 0.00157\,B*D \\ & + 0.290\,B*E + 0.230\,C*E \end{aligned}$$

**(a)**

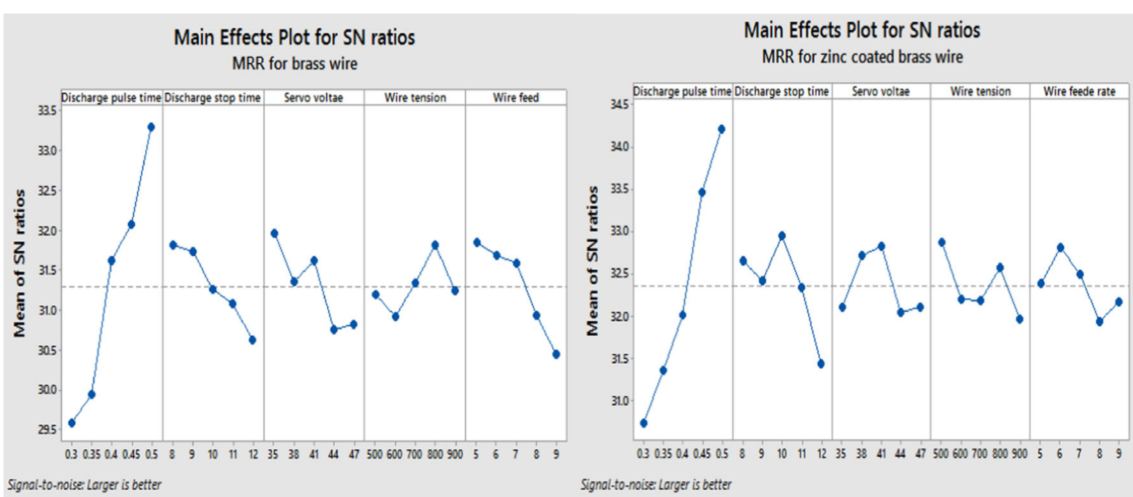


**Fig. 4** **a** Effects of process parameters on MRR. **b** Effects of process parameters interactions on MRR [Brass wire]. **c** Effects of process parameters interactions on MRR [Zinc coated brass wire]

**Fig. 4** (continued)

**(b)**

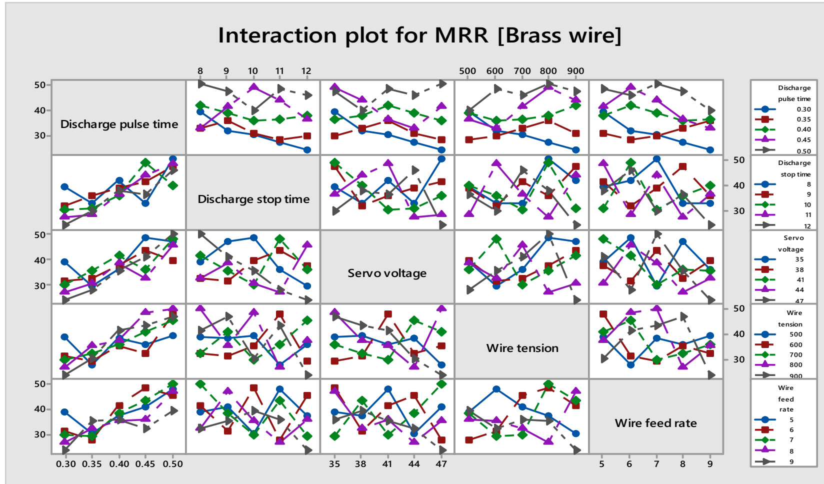


**(c)**

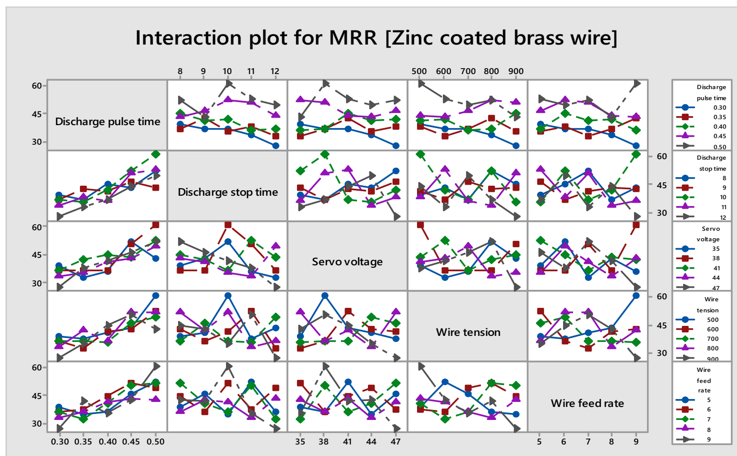


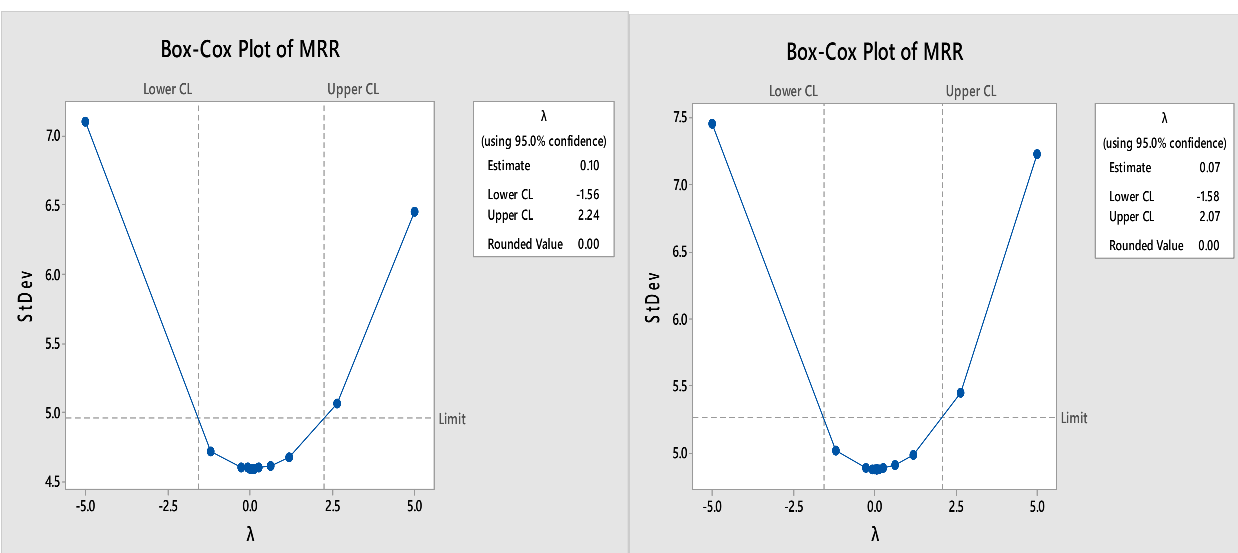


(a) Brass wire (b) Zinc coated brass wire

**Fig. 5** Box Cox plots for material removal rate

**Table 4** Analysis of variance for MRR

| Source | Brass Wire | | | | | Zinc coated brass wire | | | | |
|---|---|---|---|---|---|---|---|---|---|---|
| | Seq SS | DF | Adj MS | F-value | Percentage contribution | Seq SS | DF | Adj MS | F-value | Percentage contribution |
| Discharge pulse time | 864.79 | 4 | 216.20 | 11.02 | 67.64 | 1021.41 | 4 | 255.35 | 11.02 | 70.94 |
| Discharge stop time | 69.37 | 4 | 17.34 | 0.88 | 5.43 | 141.40 | 4 | 35.35 | 1.53 | 9.82 |
| Servo voltage | 86.79 | 4 | 21.70 | 1.11 | 6.79 | 69.42 | 4 | 17.36 | 0.75 | 4.82 |
| Wire tension | 50.31 | 4 | 12.58 | 0.64 | 3.93 | 61.57 | 4 | 15.39 | 0.66 | 4.28 |
| Wire feed rate | 128.80 | 4 | 32.22 | 1.64 | 10.08 | 53.20 | 4 | 13.30 | 0.57 | 3.70 |
| Error | 78.6 | 4 | 19.61 | | | 92.72 | 4 | 23.18 | | |
| Total | 1278.61 | 24 | | | | 1439.72 | 24 | | | |

$$MRR_{\text{Zinc coated}} = 113 - 341\,A + 30.7\,B - 7.8\,C - 0.019\,D + 0.5\,E + 211\,A*A - 1.696\,B*B + 0.034\,C*C + 0.000096\,D*D - 0.509\,E*E + 11.5\,A*B + 8.10\,A*C - 0.222\,A*D - 3.9\,A*E - 0.00248\,B*D - 0.099\,B*E + 0.220\,C*E$$

$$\text{Machining time}_{\text{brass wire}} = -7.0 + 38.9\,A + 0.09\,B - 0.147\,C + 0.0262\,D - 1.41\,E - 16.2\,A*A + 0.0150\,B*B + 0.00705\,C*C - 0.000011\,D*D + 0.0109\,E*E - 0.15\,A*B - 0.942\,A*C - 0.0170\,A*D + 2.62\,A*E - 0.000428\,B*D + 0.0096\,B*E + 0.0044\,C*E$$

$$\text{Machining time}_{\text{Zinc wire}} = -9.2 + 77.8\,A - 4.08\,B + 0.410\,C + 0.0290\,D - 0.06\,E - 24.0\,A*A + 0.1850\,B*B + 0.00581\,C*C - 0.000019\,D*D - 0.0211\,E*E - 0.96\,A*B - 1.541\,A*C - 0.0103\,A*D + 2.05\,A*E + 0.000326\,B*D + 0.0743\,B*E - 0.0349\,C*E$$

$$R_{a\ \text{Brass}} = 54.5 - 114.5\,A - 5.94\,B - 0.66\,C + 0.0191\,D + 1.13\,E + 75.0\,A*A + 0.1738\,B*B + 0.0121\,C*C - 0.000015\,D*D - 0.0446\,E*E + 6.67\,A*B - 0.422\,A*C + 0.0057\,A*D + 0.72A*E + 0.000068\,B*D - 0.0164\,B*E - 0.0150\,C*E$$

$$R_{a\ \text{Zinc wire}} = 3.2 + 5.4\,A + 0.02\,B - 0.144\,C + 0.0083\,D - 0.32\,E - 10.6\,A*A - 0.0032\,B*B + 0.0003\,C*C - 0.000004\,D*D + 0.0138\,E*E + 0.27\,A*B + 0.110\,A*C - 0.0070A*D + 0.12\,A*E + 0.000067\,B*D - 0.0268\,B*E + 0.0093\,C*E$$

Residual analysis is the major analytic device to ensure the model sufficiency. From Fig. 6, it can be comprehended that every one of the information take after a typical dispersion as every one of the focuses were set close to the straight line. Here, the standardized residual distribution seeks after that the free examples are typically put on each side of the reference line. Comparable kind of nature is likewise watched for machining time and surface roughness (Figs. 7 and 8).

## 4.2 Influence of Hardfaced Layer Thickness on WEDM Performance

Experiments were conducted to discover the impact of different hardfaced layer thickness on WEDM performance. Considering the results of existing literature [31], it is practical that the hardness of the hardfaced surface increments when the hardfacing layer thickness expanded. This might be perceived to the way that the dilution rate of the top surface diminished when the hardfacing thickness expanded. Dilution from the substrate material is more in the main layer of the store and consequently, its hardness is lower. Amid the affidavit of the second layer, the liquid metal blended with the re-dissolved diluted first layer of the store and consequently, the impact of dilution is decreased and on the resulting testimony, the dilution level lessened further [32].

For 4 mm hard-faced layer thickness, experimental results for both the wires are shown in Table 5. The variation of MRR with respect to the different hardfaced layer thickness (3 mm and 4 mm) has been shown in Fig. 9a. It is interesting to note that hardfaced layer thickness has very little effect on the MRR in WEDM. In light of Luo's [33] finding that the electrical vitality accessible for material expulsion is consistently appropriated along the length of the wire and the material evacuation rate ought not to be influenced by the material thickness. Since, there is no mechanical contact between the work piece and the electrode, material of any hardness can be machined the length of it is adequately electrically conductive. The tests,

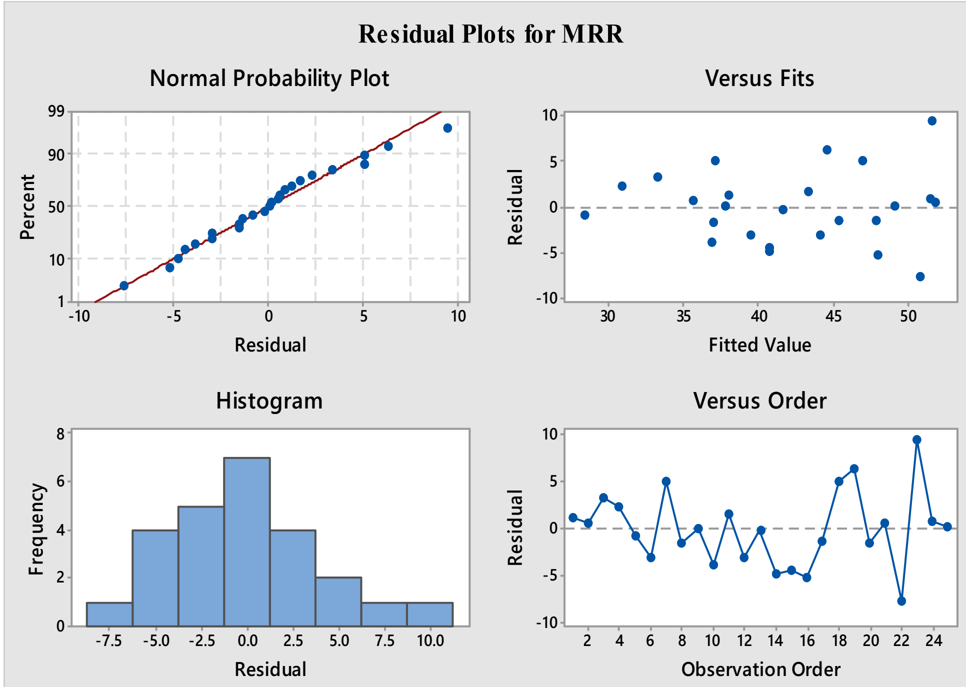


**Fig. 6** Plot of residuals of material removal rate

be that as it may, demonstrate a decline in MRR for bigger hardfaced layer thickness, which is in all probability brought on by insufficient flushing because of the more extended kerf region. This is an agreement with other researchers [34]. Practically comparable graphical practices have been observed for zinc-coated wire (Fig. 10a).The range of MRR with zinc coated wire is higher than brass wire. The low melting temperature of wire enhances the spark development and decline dielectric ionization time. In this way, the MRR increases [35]. Hence, machining time is less with zinc coated brass wire (Fig. 10b).

Figures 9c and 10c represent the consequence of hardfaced layer thickness on surface roughness in WEDM. The inverse impact is the aftereffect of decreased surface roughness with

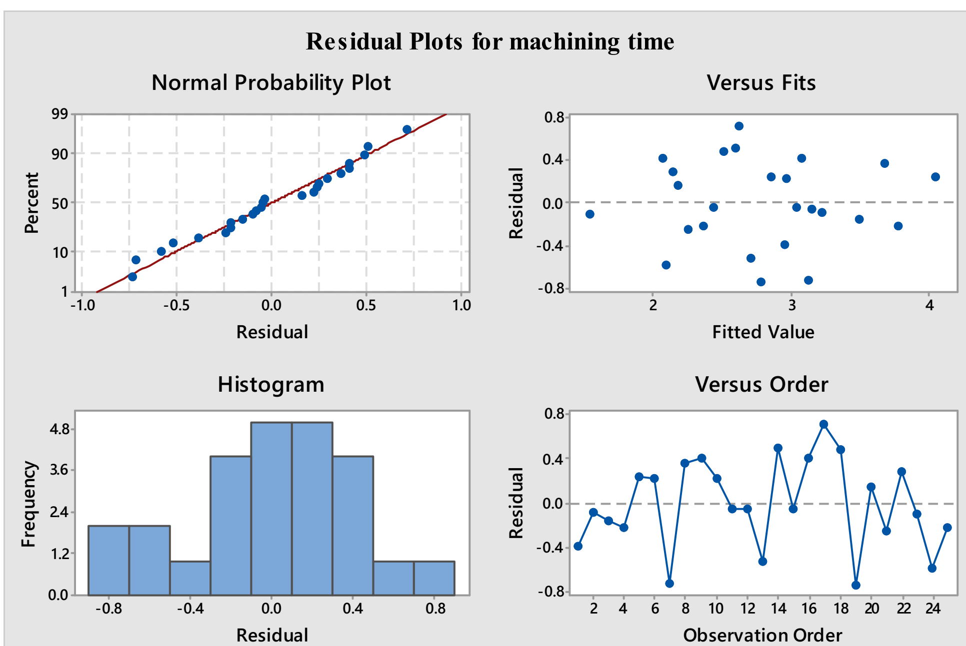


**Fig. 7** Plot of residuals of machining time

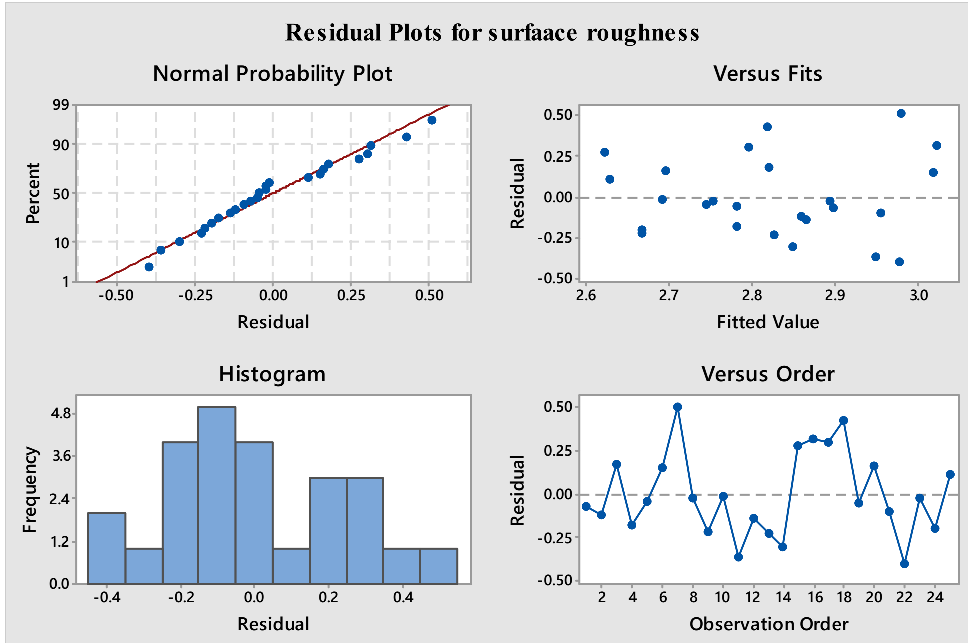


**Fig. 8** Plot of residuals of surface roughness

**Table 5** Experimental results for WEDM performance [hardfaced layer thickness is 4 mm]

| Experiment No. | Brass wire | | | Zinc coated brass wire | | |
|---|---|---|---|---|---|---|
| | *MRR* | Machining time | $R_a$ | *MRR* | Machining time | $R_a$ |
| 1 | 38.668 | 2.63 | 3.02 | 38.656 | 2.66 | 2.71 |
| 2 | 30.490 | 3.57 | 2.91 | 34.900 | 3.28 | 2.54 |
| 3 | 29.421 | 4.03 | 2.68 | 35.888 | 3.44 | 2.92 |
| 4 | 26.461 | 4.61 | 2.02 | 32.621 | 3.75 | 2.46 |
| 5 | 24.611 | 5.22 | 2.44 | 26.099 | 4.51 | 2.66 |
| 6 | 31.428 | 3.38 | 2.28 | 34.643 | 3.39 | 3.08 |
| 7 | 34.627 | 3.57 | 2.45 | 40.245 | 2.75 | 3.17 |
| 8 | 29.922 | 4.41 | 2.07 | 34.245 | 4.19 | 2.26 |
| 9 | 27.575 | 4.49 | 2.17 | 35.030 | 3.93 | 2.19 |
| 10 | 29.976 | 3.71 | 2.27 | 32.002 | 3.37 | 2.47 |
| 11 | 41.409 | 3.17 | 2.33 | 42.873 | 3.24 | 2.16 |
| 12 | 37.151 | 3.15 | 1.79 | 40.975 | 2.71 | 2.48 |
| 13 | 34.357 | 4.89 | 2.71 | 40.334 | 2.50 | 2.44 |
| 14 | 34.755 | 3.62 | 2.69 | 35.622 | 3.44 | 2.26 |
| 15 | 35.331 | 3.31 | 2.99 | 35.599 | 3.36 | 2.73 |
| 16 | 32.167 | 3.56 | 2.28 | 41.556 | 2.83 | 3.28 |
| 17 | 40.634 | 3.03 | 2.96 | 44.957 | 3.72 | 2.79 |
| 18 | 48.120 | 2.67 | 2.74 | 49.324 | 3.06 | 2.91 |
| 19 | 42.804 | 2.86 | 2.50 | 48.113 | 2.14 | 2.68 |
| 20 | 36.173 | 3.40 | 3.34 | 43.033 | 2.81 | 2.59 |
| 21 | 48.345 | 2.38 | 2.45 | 51.433 | 2.14 | 2.67 |
| 22 | 46.828 | 2.82 | 3.10 | 42.115 | 2.91 | 2.34 |
| 23 | 38.885 | 3.17 | 2.60 | 58.351 | 1.71 | 2.54 |
| 24 | 47.633 | 2.59 | 3.37 | 51.096 | 1.68 | 2.19 |
| 25 | 45.324 | 2.43 | 5.87 | 49.075 | 2.56 | 2.63 |

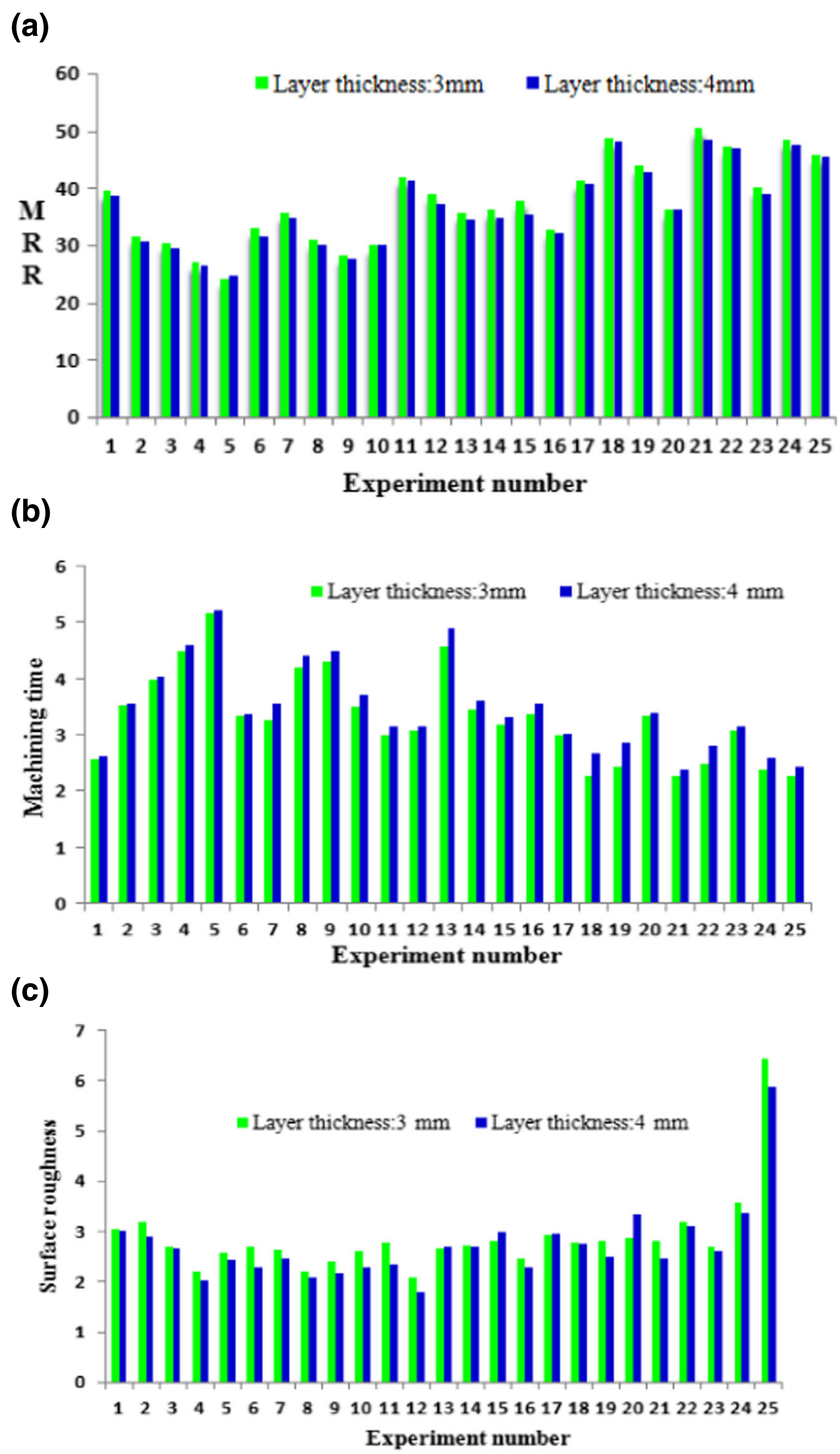


**Fig. 9** Influence of different hardfaced layer thickness on WEDM performance for brass wire

expanded layer thickness. The expanded engagement length causes a decrease in spark vitality circulation, which produces littler and all the more exceptionally distributed discharge. In Fig. 9c, abrupt change in the surface roughness value (trail no. 25) has been occurred due to welding defects viz. porosity, blow holes, cracking etc. which may results in non-uniform distribution of hardfacing over the parent metal and may lead to wire breakage during WEDM of hardfacing alloy.

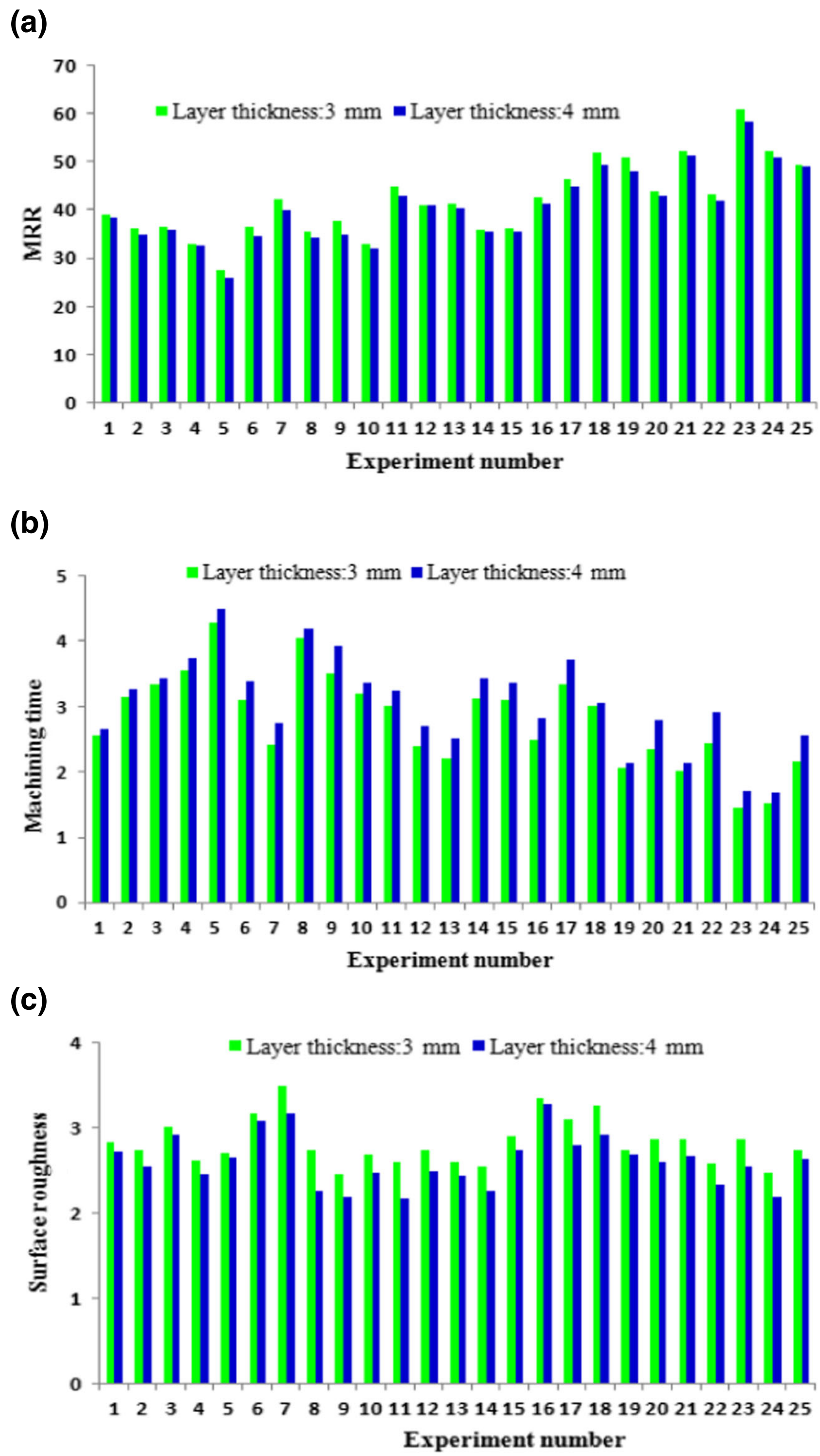


**Fig. 10** Influence of different hardfaced layer thickness on WEDM performance for zinc coated brass wire

## 5 Conclusions

The impact of different input process parameters on WEDM performance characteristics has been investigated. It additionally highlights the application of hybrid multi-criteria decision making approach such as TOPSIS in combination with PCA to recognize optimal process parameters. Investigational outcome and conclusions are as follows:

- Regression equation has been effectively used to build up the mathematical models for various performance measures.

- The important factors that influence the material removal rate for brass wire are discharge pulse time, wire feed rate and servo voltage. For zinc coated brass wire, the significant factors are discharge pulse time and discharge stop time.
- Optimum combination of input process parameters for the multiple performance distinctiveness should be preferred as $A_1B_5C_5D_5E_5$ (brass wire) and $A_2B_3C_4D_5E_1$ (Zinc coated brass wire).
- Based on Taguchi's plan of examination, it can be reasoned that the hardfaced layer thickness has little impact on the material removal rate in WEDM. The inverse impact is the aftereffect of decreased surface roughness with expanded layer thickness.
- The exploratory outcomes affirm that machining with zinc coated brass wire contrasted with brass wire prompts bring down surface roughness and machining time, and higher MRR in WEDM.

Supplementary investigate might endeavor to think about the other hardfacing techniques. SEM analysis of WED-machined surface and surface topography is another significant area in which research work can be carried out. The above research issues will be dealt in the next paper.

## References


1. Liu D, Liu R, Wei Y, Zhu K (2013) Microstructure and wear properties of Fe-15Cr-2.5 Ti-2C-xB wt% hardfacing alloys. Appl Surf Sci 271:253–259
2. Io SI, Just C, Xhiku F (2012) Optimisation of multiple quality characteristics of hardfacing using grey-based Taguchi method. Mater Des 33:459–468
3. Karabasov YS (2002) New materials. Moscow Institute of Steel and Alloys, Moscow
4. Kuznetsov MA, Zernin EA (2012) Nanotechnologies and nanomaterials in welding production. Welding Int 26:311–313
5. Majumder H, Maity KP (2018) Predictive analysis on responses in WEDM of titanium grade 6 using General Regression Neural Network (GRNN) and Multiple Regression Analysis (MRA). Silicon. https://doi.org/10.1007/s12633-017-9667-1
6. Soni H, Narendranath S, Ramesh MR (2018) Effects of wire electro-discharge machining process parameters on the machined surface of Ti50Ni49Co1Shape memory alloy. Silicon. https://doi.org/10.1007/s12633-017-9687-x
7. Soni H, Narendranath S, Ramesh MR (2018) Experimental investigation on effects of wire electro discharge machining of Ti50Ni45Co5 shape memory alloys. Silicon https://doi.org/10.1007/s12633-018-9780-9
8. Majumder H, Maity KP (2018) Prediction and optimization of surface roughness and micro-hardness using GRNN and MOORA-fuzzy-a MCDM approach for nitinol in WEDM. Measurement 118:1–13
9. Majumder H, Maity KP (2017) Optimization of machining condition in WEDM for titanium grade 6 using MOORA coupled with PCA—a multivariate hybrid approach. J Adv Manuf Syst 16:81
10. Mahapatra SS, Patnaik A (2007) Optimization of wire electrical discharge machining (WEDM) process parameters using Taguchi method. Int J Adv Manuf Technol 34(9–10):911–925
11. Bobbili R, Madhu V, Gogia AK (2013) Effect of wire-EDM machining parameters on surface roughness and material removal rate of high strength armor steel. Mater Manuf Process 28(2):364–368
12. Dhobe MM, Chopde IK, Gogte CL (2014) Optimization of wire electro discharge machining parameters for improving surface finish of cryo-treated tool steel using DOE. Mater Manuf Process 29:1381–1386
13. Fonda P, Katahira K, Yamazaki K (2012) WEDM condition parameter optimization for PCD microtool geometry fabrication process and quality improvement. Int J Adv Manuf Technol 63:1011–1019
14. Kumar A, Kumar V, Kumar J (2014) Microstructure analysis and material transformation of pure titanium and tool wear surface after wire electric discharge machining process. Mach Sci Technol 18:47–77
15. Li L, Li ZY, Wei XT, Cheng X (2015) Machining characteristics of Inconel 718 by sinking-EDM and wire-EDM. Mater Manuf Process 30(8):968–973
16. Mandal A, Dixit AR, Das AK, Mandal N (2015) Modeling and optimization of machining Nimonic C-263 super alloy using multicut strategy in WEDM. Mater Manuf Process 31(7):860–868
17. Manjaiah M, Narendranath S, Basavarajappa S, Gaitonde VN (2015) Effect of electrode material in wire electro discharge machining characteristics of $Ti_{50}Ni_{50-x}Cu_x$shape memory alloy. Precis Eng 41:68–77
18. Shyam L, Sudhir K, Khan ZA, Siddiquee AN (2013) Wire electrical discharge machining of AA7075/SiC/Al2O3 hybrid composite fabricated by inert gas-assisted electromagnetic stir-casting process. J Braz Soc Mech Sci Eng 36(2):335–346
19. Shayana AV, Afzac RA, Teimourib R (2013) Parametric study along with selection of optimal solutions in dry wirecut machining of cemented tungsten carbide (WC-Co). J Manuf Process 15(4):644–658
20. Nikalje AM, Kumar A, Sai KVS (2013) Influence of parameters and optimization of EDM performance measures on MDN 300 steel using Taguchi method. Int J Adv Manuf Technol 69:41–49
21. Zhang GJ, Zhang Z, Guo JW, Ming WY, Li MZ, Huang Y (2013) Modelling and optimization of medium-speed WEDM process parameters for machining SKD11. Mater Manuf Process 28(10):1124–1132
22. Bhangoria JL, Puri YM (2010) Kerf width analysis for wire cut electro discharge machining of SS304 L using design of experiments. Ind J Sci Technol 3(4):369–373
23. Tosun N (2003) The effect of the cutting parameters on performance of WEDM. KSME Int J 17(6):816–824
24. Tosun N, Cogun C, Tosun G (2004) A study on kerf and material removal rate in wire electrical discharge machining based on Taguchi method. J Mater Process Technol 152:316–322
25. Ahmed LS, Kumar MP (2016) Multiresponse optimization of cryogenic drilling on Ti-6Al-4 V alloy using TOPSIS method. J Mech Sci Technol 30(4):1835–1841
26. Kalayarasan M, Murali M (2016) Optimization of process parameters in EDM using Taguchi method with grey relational analysis and TOPSIS for ceramic composites. Int J Eng Res Afr 22:83–93
27. Şimşek B, İç YT, Şimşek EH (2013) A TOPSIS-based Taguchi optimization to determine optimal mixture proportions of the high strength self-compacting concrete. Chemom Intell Lab Syst 125:18–32

28. Saha A, Mondal SC (2016) Experimental investigation and modelling of WEDM process for machining nano-structured hardfacing material. J Braz Soc Mech Sci Eng 39:3439–3455
29. Saha A, Mondal SC (2016) Multi-objective optimization in WEDM process of nanostructured hardfacing materials through hybrid techniques. Measurement 94:46–59
30. Saha A, Majumder H (2016) Multi criteria selection of optimal machining parameter in turning operation using comprehensive grey complex proportional assessment method for ASTM A36. Int J Eng Res Afr 23:24–32
31. Fouilland L, Mansori MEI, Gerland M (2007) Role of welding process energy on the microstructural variations in a cobalt base superalloy hardfacing. Surf Coat Technol 201(14):6445–6451
32. Das CR, Albert SK, Bhaduri AK, Sudha C, Terrance ALE (2005) Characterization of nickel based hardfacing deposits on austenitic stainless steel. Surf Eng 21:29–290
33. Luo YF (1995) Energy-distribution strategy in fast-cutting wire EDM. J Mater Process Technol 55(3–4):380–390
34. Shah A, Mufti NA, Rakwal D, Bamberg E (2011) Material removal rate, kerf, and surface roughness of tungsten carbide machined with wire electrical discharge machining. J Mater Eng Perform 20(1):71–76
35. Kuriakose S, Shunmugam MS (2004) Characteristics of wire-electro discharge machined Ti6Al4 V surface. Mater Lett 58:2231–2237